Research Article

Jianfen Kang, Yanfeng Guo*, Yungang Fu, Qiong Li, and Yabo Lv

Cushioning energy absorption of paper corrugation tubes with regular polygonal cross-section under axial static compression

https://doi.org/10.1515/secm-2021-0003
Received Aug 19, 2018; accepted Feb 27, 2019

Abstract: The paper corrugation tube is an innovative kind of energy absorbing structure and shock absorber which can play an important role on the cushioning energy absorption for airdrop equipments and transportation packaging. The deformation characteristics and failure modes of the regular triangle, quadrangle, pentagon and hexagon paper corrugation tubes were comparatively studied by a series of axial static compression experiments, the cushioning energy absorption was evaluated by the seven characteristic parameters (*e.g.* initial peak force, mean crush force, total energy absorption, specific energy absorption, crush force efficiency, unit area energy absorption and stroke efficiency), and the influences of tube direction, cross-sectional shape, tube length and compression rate on failure modes and cushioning energy absorption were analyzed and compared. These researches showed that the tubes along X direction only have the accordion deformation mode, yet the tubes along Y direction have four deformation modes including steady state progressive buckling, Euler buckling, angular tear and transverse shear. For the paper corrugation tubes along Y direction, the cross-sectional shape has obvious influence on the cushioning energy absorption of structures, and the specific energy absorption and unit area energy absorption of regular triangle and pentagon tubes are better than those of the tubes with regular quadrilateral and hexagonal cross-section at compression rates of 12 and 48mm/min. The tube length of 150 mm or compression rate of 72 mm/min would cause the increase of contribution proportion of non-ideal deformation mode and the decrease of cushioning properties. The paper corrugation tubes along X direction have more stable and controllable deformation mode, yet the paper corrugation tubes along Y direction have better cushioning energy absorption.

Keywords: paper corrugation tube; axial static compression; folding model; deformation mode; cushioning energy absorption; mean crush force

1 Introduction

With the extensive application of corrugated sandwich structure in the field of packaging science and technology, the corrugated paperboard has become one of the most important non-metallic cellular sandwich structures. It could replace the traditional wooden materials and plastic foams and their packaging, which has been emphasized in protection and packaging engineering of military and civil products because of many advantages of low-cost, light weight, high strength-to-weight ratio and stiffness-to-weight ratio, attractive impact resistance and simple manufacturing process [1–4]. In the packaging protection system, the corrugated paperboard as resilient structure provides the required shock and vibration isolation between the packaged product and the container, through its own compression deformation and cushioning energy absorption to achieve product protection and safe transportation.

The typical energy absorbing structure of corrugated paperboard can be divided into two types. One type is the laminated paper corrugation structure, such as the corrugated paperboard with different layers, the folding and elastic paper corrugation structure, and the laminated plate with honeycomb paperboard or plastic foam, which can achieve cushioning energy absorbing function by transverse compression deformation. Another type is the tubular paper corrugation structure, such as the paper corrugation tube with regular polygonal cross-section. The paper corrugation tube filled with plastic foam, which can reduce the external load by axial compression deforma-

***Corresponding Author: Yanfeng Guo:** Faculty of Printing, Packaging Engineering and Digital Media Technology, Xi'an University of Technology, Xi'an 710048, Shaanxi Province, China; Email: guoyf@xaut.edu.cn
Jianfen Kang, Yungang Fu, Qiong Li, Yabo Lv: Faculty of Printing, Packaging Engineering and Digital Media Technology, Xi'an University of Technology, Xi'an 710048, Shaanxi Province, China

tion. More studies have been conducted on bearing capacity and energy absorption of the laminated paper corrugation structure. For example, Lu *et al.* [5] adopted curved beam element and bilinear constitutive model to study the compressive responses and failure mechanisms of single-wall corrugated paperboards with B- and C-type at different static compression rate, and proved that the corrugated parameter and compression rate have apparent controlling effect on the overall deformation and local collapse. Krusper *et al.* [6] proposed a simplified analytical model for calculating the nonlinear deformation of single-wall corrugated paperboard during out-of-plane compression by using linear elastic and engineering beam theory and beam elements including large deflections and large rotations. Rami and Talbi *et al.* [7, 8] studied the mechanical behaviors of corrugated paperboard such as buckling, stability, collapse and ultimate failure by using some finite element models and commercial finite element code ABAQUS or ANSYS. Sek *et al.* [9, 10] analyzed the cushioning properties and its predictive model, vibration transmissibility and frequency response of single-wall corrugated paperboard, and investigated the quasi-static and dynamic compression curves of multi-layered corrugated paperboard. Gao *et al.* [11] studied the impact response and cushioning properties of B-type double-wall corrugated paperboard at different drop-shocks, and proposed a nonlinear viscoelastic plastic model of dynamic compression strain. Zhu *et al.* [12] identified dynamic property parameters of corrugated paperboard considering viscoelasticity under the shock load condition by Prony method. Wang *et al.* [13] experimentally investigated the static cushioning properties and energy absorption of corrugated sandwich paperboards of B, C, E, BE, CE, and BC types, and the increase of base paper thickness or the decrease of the corrugated paperboard size can increase the relative density and improve the cushioning properties. Guo *et al.* [14–16] studied the drop impact cushioning curves of X-PLY corrugated paperboard and the structures of elastic-type and folding-type, and indicated that these laminated paper corrugation structures appear the deformation mode with a layer by layer collapse and have excellent cushioning energy absorbing property. Moreover the deformation and energy absorption of multi-layered aluminum corrugated sandwich panel under low velocity impact also were focused [17].

In recent years, considering the advantage of corrugated structure which is much easier to bend under axial compression, the corrugated tubular structure of metal or composite material was proposed by researchers to effectively improve the bearing capacity and energy absorption of thin-walled tubular structure [18]. For example, Eyvazian *et al.* [19] experimentally studied the cushioning energy absorption of parallel and laterally corrugated circular aluminum tubes with five geometrical types, and proved corrugated aluminum tube has significantly improved the controllability, energy absorption mechanism and collapse modes of circular tubes under the axial load. Liu *et al.* [20] focused on the axial-impact buckling modes and energy absorbing properties of thin-walled corrugated aluminum tubes with sinusoidal patterns, and the theoretical prediction and numerical simulations indicated that the corrugated tube has controllable and preferable energy absorbing properties. Xiong *et al.* [21] studied the quasi-static axial compressive mechanical properties of longitudinal and circumferential carbon fiber composite corrugated sandwich cylindrical shell with the classic shell buckling theory, and obtained four kinds failure modes of Euler buckling, global buckling, local buckling and panel crushing. Kılıçaslan *et al.* [22] investigated the crushing responses and energy absorbing properties of Al foam-filled corrugated aluminum alloy single- and double-tube, and analyzed the influence of geometric parameters such as radius of inner tube and wall thickness of inner tube on energy absorbing capacity.

The paper corrugation tubular structures can improve the energy absorbing property for airdrop equipments and transportation packaging through the absorbing energy of plastic deformation. In this paper, we put forward an innovative kind of energy absorbing structure and shock absorber, the regular polygon (*e.g.* regular triangle, quadrangle, pentagon and hexagon) paper corrugation tubes, and made comparative analyses of their compression deformation characteristics and failure modes by a series of axial static compression experiments. Then the cushioning energy absorption of paper corrugation tube has been studied and evaluated by the seven characteristic parameters (*e.g.* initial peak force, mean crush force, total energy absorption, specific energy absorption, crush force efficiency, unit area energy absorption and stroke efficiency), and the influences of different tube direction, cross-sectional shape, tube length, and compression rate on failure modes and cushioning energy absorption were discussed. These research works can provide the theoretical and technical basis for the development and application of regular polygon paper corrugation tubes.

Table 1: Basic parameters of the BC-type corrugated paperboard

Materials	Grammage (g/m^2)	Thickness (mm)	Tensile strength (N/mm^2)		Ring crush test (kN/m)	
			Cross direction	Machine direction	Cross direction	Machine direction
Face/Inner sheet	180	0.24	15.5	38.5	1.583	1.934
Corrugation core	140	0.28	11.0	20.0	0.904	1.098

2 Experimental materials and test method

2.1 Experimental materials

The paper corrugation tubes with the regular trilateral, quadrilateral, pentagonal, hexagonal cross-sections are also made of BC-type corrugated paperboard by machining technology of cutting, indentation, folding and full lapped adhesion. All cross-sectional side lengths are 50 mm and the full lapped adhesion of the paper corrugation tubes as shown in Figure 1. The BC-type corrugated paperboard consists of two layers of corrugation core sandwiches, two face sheets and one inner sheet. The corrugation core sandwiches are corrugated paper, and the face sheets and inner sheet are kraft linerboard paper. The basic parameters of the BC-type corrugated paperboard are given in Table 1. The thickness of the BC-type corrugated paperboard is 7.0 mm and the edge crush test is 6771 N/m. The geometric parameters of paper corrugation tubes include tube direction, tube length and cross-sectional shape.

The numbering of the specimens is named Cn-l-v-d, C indicates corrugated paperboard, n is the number of cross-sectional side, l refers to the length (70, 110, 150 mm, mainly in 110mm), v refers to the compression rate (including 12, 48 and 72 mm/min), d is the axial direction of paper corrugation tube (X and Y directions). The paper corrugation tube along X direction means that the axial direction of tube is parallel to MD direction of the corrugated paperboard, as shown in Figure 2(a). The paper corrugation tube along Y direction is parallel to CD direction of the corrugated paperboard, as shown in Figure 2(b). For example, "C5-110-12-X" means that the regular pentagon paper corrugation tube along X direction with the tube length of 110mm is compressed axially at compression rate of 12 mm/min.

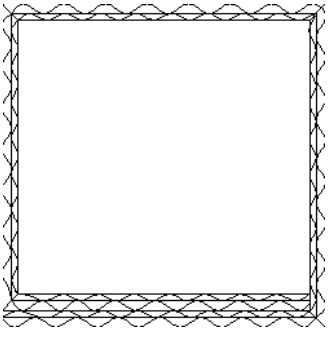

Figure 1: Full lapped adhesion of paper corrugation tubes

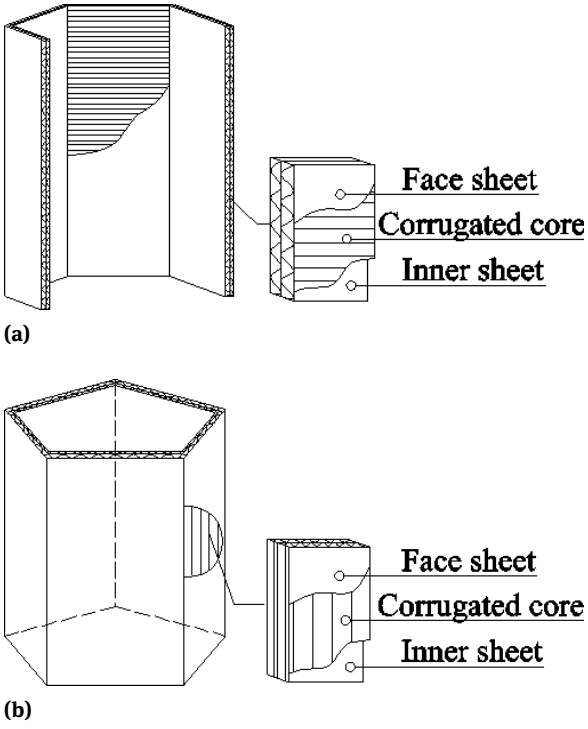

Figure 2: Geometry representation of paper corrugation tubes: (a) tubes along X direction; (b) tubes along Y direction

2.2 Test method of axial static compression

Before the test, all specimens were preconditioned to equilibrium in air uniformly maintained for at least 24 hours at ambient temperature 20°C and relative humidity 65%. The test method is in accordance with the ASTM D 1225 "Standard test method for flat crush resistance of corrugated fiberboard" and GB 8168 "Testing method of static

compression for package cushioning materials" (Chinese National Standard). The mount and fixture of the specimen are displayed in Figure 3. The specimen was mounted in the center of the fixed rigid platen of computer servo control materials testing systems (HT-2402, Hung Ta Instrument Co., Ltd. Taiwan, China), and then the moving rigid platen compressed along the axial direction of specimen at a controllable constant rate. During the compression tests, the compression load was exerted on the specimens by the moving rigid platen of the package compression tester, and the platen was controlled with three kinds of compression rate of 12, 48 and 72 mm/min. The compression load and the vertical displacement could be read and recorded by the testing apparatus. After the specimen of paper corrugation tube reached a structural failure, the static compression test ended. Then the cushioning energy absorption parameters of the paper corrugation tubes with different tube directions, tube lengths, cross-sectional shapes and compression rates were calculated according to the recorded experimental data of the compression load and the vertical displacement.

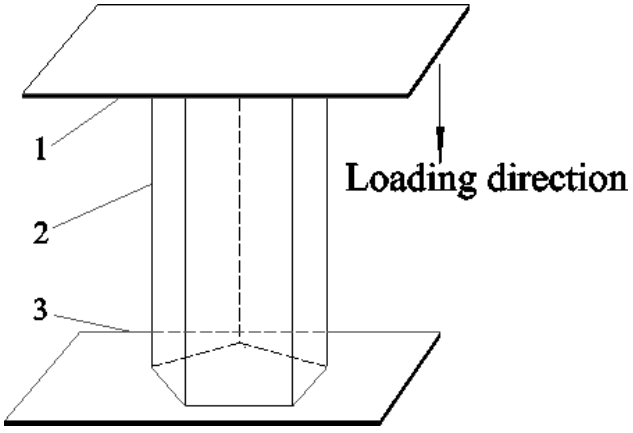

Figure 3: Mount and fixture of specimens: 1.Moving rigid platen; 2.Specimen; 3.Fixed rigid platen

3 Experimental results

3.1 Compression deformation modes

(1) For the axial static compression, the paper corrugation tube along X direction has only the accordion deformation mode is shown in Figure 4. This mode has excellent stability and controllability because the axial compression load is applied along the direction of corrugation wave of corrugated paperboard and the sinusoidal peaks and troughs of the corrugation cores are sources of plastic hinge. At the beginning of compression, the paper corrugation tube along X direction appeared a folding deformation at the bottom or top. With the deformation increasing, the structure forms periodical folding units along the MD direction of the corrugated paperboard. Moreover, this deformation is similar to the spring compression mode, and the partial deformation can be recovered after the compression load removed.

Figure 4: Deformation mode of paper corrugation tube along X direction

(2) The deformation modes of the paper corrugation tubes along Y direction are shown in Figure 5. For an example of the regular pentagon paper corrugation tube, the analyses of the deformation modes of tubes along Y direction are displayed in Figure 6. The deformation modes of the tubes along Y direction can be classified into four types including steady state progressive buckling, Euler buckling, angular tear and transverse shear. It is mainly the mixture of the ideal deformation mode of steady state progressive buckling and the other one or multiple non-ideal deformation modes.

Figure 5: Deformation modes of paper corrugation tubes along Y direction

The steady state progressive buckling occurs firstly when the paper corrugation tubes along Y direction are compressed. The separated deformation occurs between

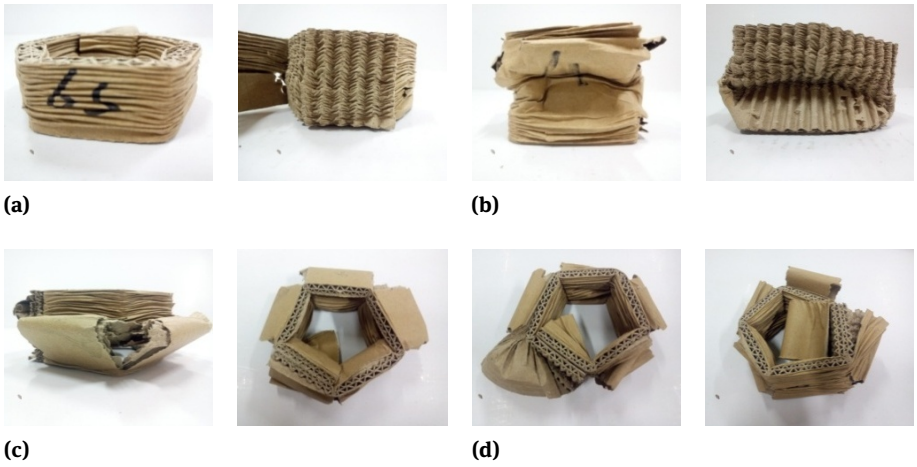

Figure 6: Deformation modes of regular pentagon paper corrugation tube along Y direction: (a) steady state progressive buckling; (b) Euler buckling; (c) angular tear; (d) transverse shear

corrugation core and face sheets because of their different arrangement. The corrugation core forms periodical folding deformation along the corrugation pillar of corrugated paperboard, and the face sheets emerges the layered folding deformation in Figure 6(a). The deformation of Euler buckling is shown in Figure 6(b). For the part of Euler buckling, only the bending part appears plastic hinge, the corrugation core and the face sheets form buckling folding together. Meanwhile the non-bending part has no deformation and no plastic hinge. As the changes of cross-sectional shape, tube length and compression rate, the paper corrugation tubes along Y direction would appear different degree deformations of angular tear or transverse shear. From the deformation mode of Figure 6(c), it can be seen that the angular tear along the corner line form a transitional plastic hinge on the surface and the rest part have no changes, the angular tear would greatly decrease the cushioning capacity of paper corrugation tube. In addition, the transverse shear deformation is caused by the shearing force acting on the wall of paper corrugation tube, and the delamination between the corrugation core and the face sheets of double-wall corrugated paperboard would appear. During the axial static compression, no periodical folding compression occurs after the face sheets are delaminated, but the plastic hinge of the corrugation core along the corrugation pillar is produced as Figure 6(d).

3.2 Cushioning energy absorbing characteristics

There are seven significant parameters adopted to evaluate the cushioning energy absorbing characteristics of paper corrugation tubes, *i.e.*, initial peak force (P_{max}), mean crush force (P_{mean}), total energy absorption (E), specific energy absorption (SEA), crush force efficiency (CFE), unit area energy absorption (S), stroke efficiency (SE) [19, 20].

(1) The total energy absorption is calculated through the direct numerical integration of the load and displacement curve before the densification of structure, as follows:

$$E = \int_0^{\delta} P\mathrm{d}s \tag{1}$$

where P and δ are the static pressure and the crush length, respectively.

(2) The mean crush force is defined as the ratio of the total energy absorption to the crush length, as follows:

$$P_{mean} = \frac{E}{\delta} = \frac{\int_0^{\delta} P\mathrm{d}s}{\delta} \tag{2}$$

(3) The crush force efficiency is defined as the ratio of the mean crush force to the initial peak force. For an ideal energy absorbing structure, the value of CFE is 100%.

(4) The specific energy absorption is defined as the ratio of the total energy absorption to the mass of specimen, as follows:

$$SEA = \frac{E}{m} = \frac{\int_0^{\delta} P\mathrm{d}s}{m} \tag{3}$$

where m is the gross mass of the paper corrugation tube.

(5) The unit area energy absorption is defined as the ratio of the total energy absorption before the densification

Table 2: Cushioning energy absorption of paper corrugation tubes along X direction

Specimens	P_{max} (N)	P_m (N)	*SE* (%)	*E* (J)	*SEA* (J/g)	*S* (J/cm^2)	*CFE* (%)
C3-110-12-X	1225	728	57.9	45.7	1.80	3.26	59.4
C3-110-48-X	1125	725	59.3	47.1	1.88	3.36	64.4
C3-110-72-X	1185	793	58.9	50.5	2.01	3.61	66.9
C4-110-12-X	1280	758	63.4	50.6	1.69	2.89	59.2
C4-110-48-X	1214	787	60.8	52.4	1.81	3.00	64.8
C4-110-72-X	1235	840	66.1	59.9	2.09	3.42	68.0
C5-110-12-X	1300	880	64.4	62.1	1.74	2.96	67.7
C5-110-48-X	1280	917	65.5	65.7	1.85	3.13	71.6
C5-110-72-X	1360	936	66.6	67.3	1.90	3.20	68.8
C6-110-12-X	1315	887	66.4	64.5	1.63	2.63	67.5
C6-110-48-X	1325	1011	64.8	71.5	1.75	2.92	76.3
C6-110-72-X	1175	976	69.4	73.9	1.83	3.02	83.1

Table 3: Cushioning energy absorption of paper corrugation tubes along Y direction

Specimens	P_{max} (N)	P_m (N)	*SE* (%)	*E* (J)	*SEA* (J/g)	*S* (J/cm^2)	*CFE* (%)
C3-110-12-Y	2420	2008	67.6	148.0	5.90	10.57	83.0
C3-110-48-Y	2515	2076	71.0	159.4	6.35	11.39	82.5
C3-110-72-Y	2675	2216	69.1	166.1	6.57	11.86	82.8
C4-110-12-Y	2845	2254	70.6	173.3	5.78	9.90	79.2
C4-110-48-Y	3220	2303	71.6	179.5	6.09	10.26	71.5
C4-110-72-Y	3000	2402	70.6	183.9	6.26	10.51	80.1
C5-110-12-Y	3175	2841	71.0	218.2	6.06	10.39	89.5
C5-110-48-Y	3465	2757	72.9	219.2	6.11	10.44	79.6
C5-110-72-Y	3330	2776	71.3	215.1	6.09	10.24	83.4
C6-110-12-Y	3945	2975	71.0	231.3	5.77	9.44	75.4
C6-110-48-Y	3705	3049	75.2	250.1	6.08	10.21	82.3
C6-110-72-Y	3870	3018	74.4	244.6	6.10	9.98	78.0

of structure to the bearing area, as follows:

$$S = \frac{E}{A} = \frac{\int_0^\delta P\mathrm{d}s}{A} \tag{4}$$

(6) The stroke efficiency is defined as the ratio of the crush length to the initial length of the specimen.

According to experimental data and axial static compression curves, the energy absorbing characteristic parameters of paper corrugation tubes are calculated, and the results are respectively listed in Tables 2 and 3.

4 Effect factor analyses of cushioning energy absorption

4.1 Folding Model and energy dissipation

Figure 7 show four cross-sectional shapes of paper corrugation tubes studied in present study and the initial angle $2\psi_0$ is $\pi/3$, $\pi/2$, $3\pi/5$ and $2\pi/3$, respectively. In this paper, the paper corrugation tubes with different cross-sectional shapes are decomposed into L-type units along their center of their edges. Due to full lapped adhesion, paper corrugation tubes can be divided into single L-type unit and single-double L-type unit, as shown in Figure 7.

Wierzbicki *et al.* [23] present a super folding element model for studying crushing behavior of tube under axial compression loads, as shown in Figure 8(a). This model consists of four plane trapezoidal elements, two sections of

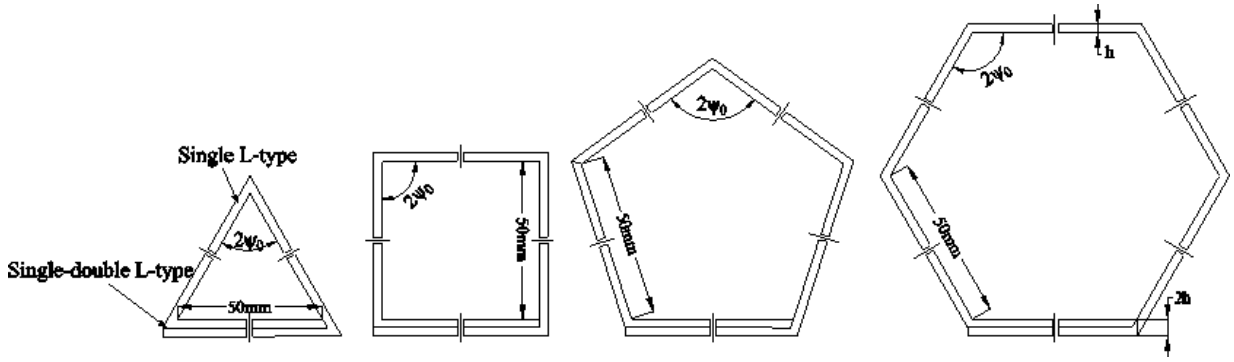

Figure 7: Cross-sectional shapes and L-type units of paper corrugation tubes

cylindrical surfaces, two sections of conical surfaces and a section of toroidal surface. The geometrical basic folding element is shown in Figure 8(b). In order to determinate the mean crush force required for the collapse of paper corrugation tubes under static loading, the energy method has been used. Neglecting the energy required for the partial breakage of full lapped adhesion, the energy dissipation is divided into three parts: (a) the extension of the toroidal shell, E_1, (b) the forming of the horizontal plastic hinge lines, E_2 and (c) the forming of the inclined plastic hinge lines, E_3.

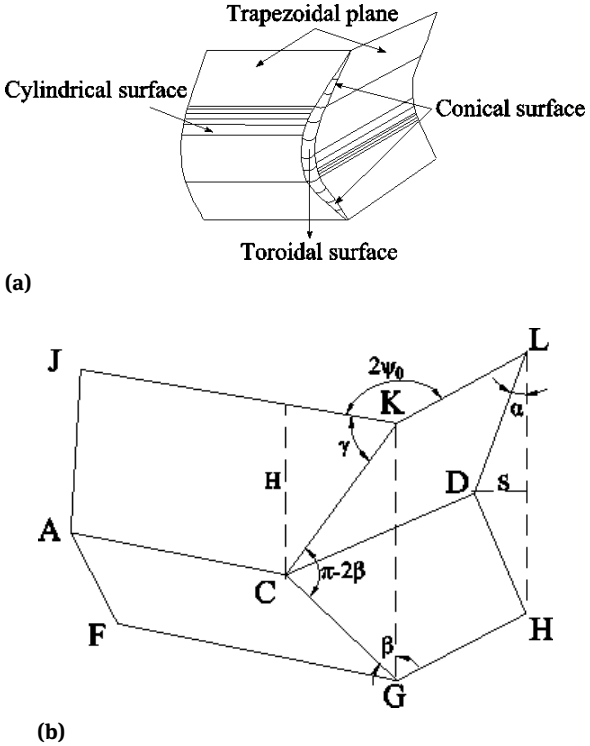

Figure 8: Folding model of an angle element: (a) basic folding element; (b) geometrical description

The plastic energy dissipation in the toroidal shell for single L-type unit can be calculated by the following equation [23]:

$$E_1' = 4HbN_0'I_1(\psi_0) = 16M_0'H\frac{b}{h}I_1(\psi_0) \tag{5}$$

and for single-double L-type unit is:

$$\begin{aligned} E_1'' &= 2HbN_0'I_1(\psi_0) + 2HbN_0''I_1(\psi_0) \\ &= 24M_0'H\frac{b}{h}I_1(\psi_0) \end{aligned} \tag{6}$$

where

$$\begin{aligned} &I_1(\psi_0) \\ &= \frac{\pi}{(\pi - 2\psi_0)\tan\psi_0}\int_0^{\pi/2}\cos\alpha\left\{\sin\psi_0\sin\left(\frac{\pi-2\psi_0}{\pi}\right)\beta\right. \\ &\left.+\cos\psi_0\left[1-\cos\left(\frac{\pi-2\psi_0}{\pi}\right)\beta\right]\right\}d\alpha, \end{aligned}$$

H is the half-wavelength of the folding element, h represents the thickness of the tubes wall, b is the radius of the cylindrical surface, σ_0 denotes the flow stress of the paper corrugation tube material. In addition, M_0 denotes the fully plastic bending moment.

For single L-type unit, there are:

$$M_0' = 1/4\sigma_0h^2, \quad N_0' = \sigma_0h \tag{7}$$

and for single-double L-type unit, then

$$M_0'' = \sigma_0h^2, \quad N_0'' = 2\sigma_0h \tag{8}$$

The relationship between flow stress and fully plastic bending moments of two kinds of L-type units are obtained:

$$M_0'' = 4M_0', \quad N_0'' = 2N_0' \tag{9}$$

The horizontal plastic hinge lines of the cylindrical surfaces can dissipate energy, and there will be two such

hinge lines in the basic folding mechanism. In this paper, the total widths C of all paper corrugation tubes are 50 mm. The contribution of this mechanism for single L-type unit is:

$$E_2' = 2M_0'C\dot{\alpha} \tag{10}$$

After the integration over the whole process:

$$E_2' = 2\int_0^{\pi/2} M_0'Cd\alpha = \pi M_0'C \tag{11}$$

yet for single-double L-type unit, then

$$E_2'' = \int_0^{\pi/2} \left(M_0'C + M_0{}''C\right) d\alpha = \frac{5\pi}{2} M_0'C \tag{12}$$

The energy dissipation in the forming of the inclined plastic hinge lines of the conical sections is:

$$\dot{E}_3' = 2M_0'L\dot{\theta} = 4M_0'\frac{H^2}{b}\frac{1}{\tan\psi_0}\frac{\cos\alpha}{\sin\gamma}\dot{\alpha} \tag{13}$$

After the integration over the whole process:

$$E_3' = 4M_0'I_3\left(\psi_0\right)H^2/b \tag{14}$$

and for single-double L-type unit, then

$$\dot{E}_3'' = M_0'L\dot{\theta} + M_0''L\dot{\theta} = 10M_0'\frac{H^2}{b}\frac{1}{\tan\psi_0}\frac{\cos\alpha}{\sin\gamma}\dot{\alpha} \tag{15}$$

$$E_3{}'' = 10M_0'I_3\left(\psi_0\right)H^2/b \tag{16}$$

In the experiments, it is assumed that the crushing distance of the mean crush force P_m is equal to $2H$ because all paper corrugation tubes have reached the stage of densification. Therefore, the total plastic work required to crush the element equals:

$$E_{ext} = 2P_mH = E_1 + E_2 + E_3 \tag{17}$$

The mechanical model of thin-walled tubes by using the folding element method is more suitable for simulating the crushing mechanism of paper corrugation tubes along X direction in the axial static compression experiment. The crumpling process of tubes along X direction is progressive, and each new fold is being formed after the previous one is completed, as shown in Figure 4. The paper corrugation tubes along Y direction are a mixture of various deformation modes and not suitable for accurate simulation with basic folding elements. For a thin-walled polygonal paper corrugation tubes along X direction with N L-type units, the energy balance equation is as follows:

$$2P_mH = \sum_{i=1}^{N-2}\left(E_1' + 2E_2' + E_3'\right) + 2\times\left(E_1'' + 2E_2'' + E_3''\right) \tag{18}$$

where N is the number of angle elements and cross-sectional side of thin-walled tube.

4.2 Effect analysis of tube direction

In order to compare the effects of tube direction on deformation mode, the typical axial static compression curves of the regular pentagon paper corrugation tubes along X and Y direction and the comparison of deformation at certain time points are given in Figure 9. The plastic plateau region of tube along X direction is much lower than that of tube along Y direction. Meanwhile, its curve fluctuation amplitude is larger, and each wave crest corresponds to plastic hinge of accordion deformation. During the whole compression, at the time of "i" moment the force reaches the initial peak load, and at the time of "ii" interval the deformation holds the stable accordion deformation stage, then at the time of "iii" moment the deformation begins to enter the densification stage. For the paper corrugation

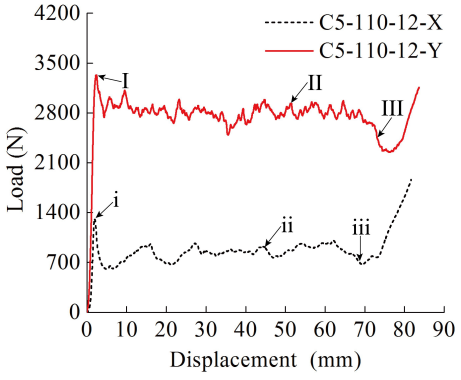

(a)

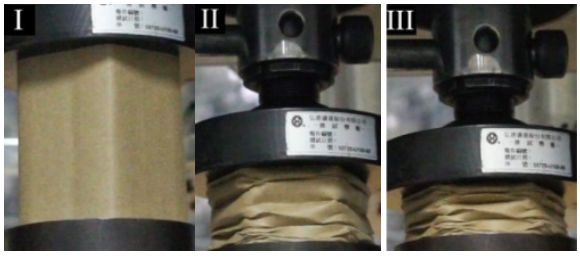

(b)

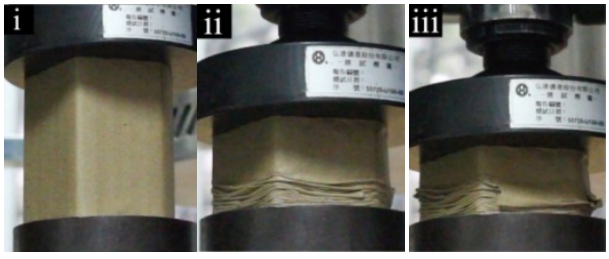

(c)

Figure 9: Axial compression of regular pentagon paper corrugation tubes: (a) load and displacement curves; (b) deformation of tube along X direction; (c) deformation of tube along Y direction

tube along Y direction, the force reaches the initial peak load at the time of "I" moment, and at the time of "II" interval the deformation is mainly the steady state progressive buckling. At the time of "III" moment, the deformations of Euler buckling and transverse shear appear and lead to the decrease of the bearing property and energy absorbing capacity.

According to the parameters of cushioning energy absorption in Tables 2 and 3, the curve swings of the tube along Y direction is relatively fine and the amplitude of swings is lower, and the bearing capacity of tube along Y direction is much higher than the tube along X direction because the axial compression load is applied along the direction of corrugation pillar for tube along Y direction but along corrugation wave for tube along X direction. Also, total energy absorption, specific energy absorption and unit area energy absorption of tubes along Y direction are higher than those of tubes along X direction. The stroke efficiency of paper corrugation tube along X direction is about 63% and the crush force efficiency is from 0.5 to 0.7. However, the stroke efficiency of the paper corrugation tube along Y direction is about 71% and the crush force efficiency is from 0.7 to 0.9.

4.3 Effect analysis of cross-sectional shape

Figures 4 and 5 show the comparison of axial compression deformation of paper corrugation tubes with different directions. For the different cross-sections, the deformation mode of tubes along X direction is stable, yet that of tubes along Y direction are a mixture of various modes. Meanwhile, the deformation becomes more complicated with the increase of side number of the regular polygon. The regular triangle tubes are mainly steady state progressive buckling and Euler buckling, and regular quadrangle tubes are mainly the combination modes of steady state progressive buckling, Euler buckling and transverse shear. The deformation modes of regular pentagon and hexagon tubes are composed of steady state progressive buckling, Euler buckling, angular tear and transverse shear. Compared with regular pentagon tubes, the regular hexagon tubes mainly appear Euler buckling and angular tear, and the degree of angular tear is more serious.

Figure 10 plots the load and displacement curves of different cross-sectional paper corrugation tubes at compression rate of 12 mm/min, and the corresponding initial peak force and mean crush force are also given in Figure 11. Combined with values of cushioning energy absorbing parameters (Tables 2 and 3), it is obvious that the increase of the cross-sectional side number of the regular polygon would leads to the increase of bearing area and gross mass of the specimens, and the initial peak force, mean crush force, total energy absorption and stroke efficiency of the paper corrugation tubes along X and Y direction all gradually increase.

The specific energy absorption, unit area energy absorption and stroke efficiency of four kinds of cross-sectional paper corrugation tube along Y direction at different compression rates are shown in Figure 12. It is clear that the specific energy absorption and unit area energy absorption of regular triangle and pentagon tubes are all larger than those of the regular quadrangle and hexagon tubes at compression rates of 12 and 48 mm/min. When the compression rate is 72 mm/min, the specific energy absorption and unit area energy absorption gradually decrease with the rise of cross-sectional side number due to the large compression rate.

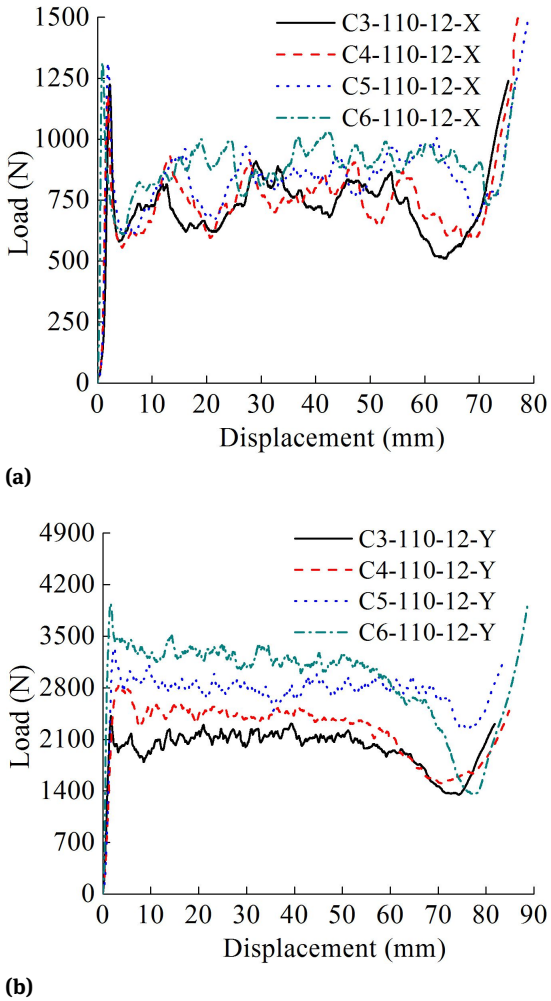

Figure 10: Load and displacement curves with different cross-sectional shapes: (a) tubes along X direction; (b) tubes along Y direction

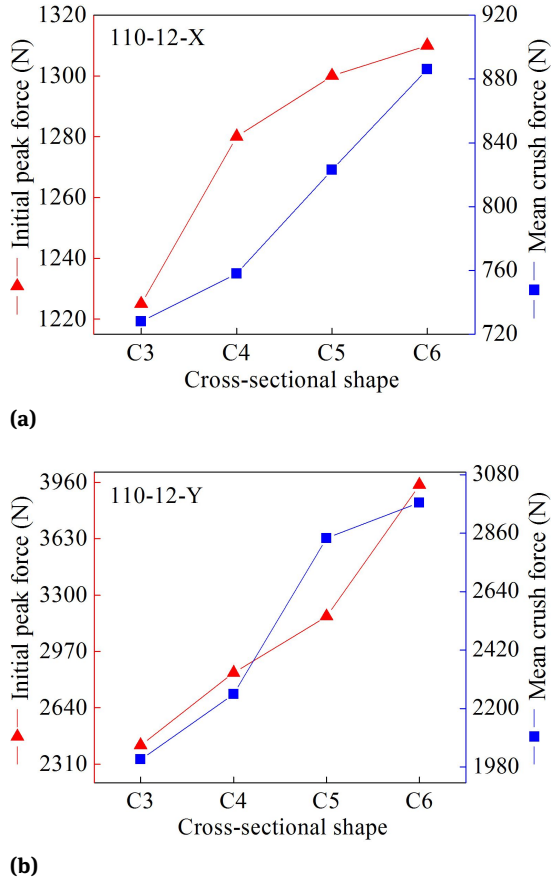

Figure 11: Initial peak force and mean crush force of paper corrugation tube: (a) tube along X direction; (b) tube along Y direction

4.4 Effect analysis of tube length

The regular pentagon paper corrugation tubes at compression rate of 12 mm/min were analyzed to determine the effects of the tube length on the deformation mode and energy absorbing performance. Its cushioning energy absorption parameters and the axial static compression curves are respectively shown in Table 4 and Figure 13. The total energy absorption, unit area energy absorption and crush force efficiency of tubes along X direction gradually rise with the increase of tube length due to the stable deformation mode, and there are no significant effects on the bearing capacity of the paper corrugation tube along X direction. However, for tubes along Y direction, it can find that for the tube length of 150 mm, the load and displacement curve has a significant descend at the end of plastic plateau region and the bearing capacity decreases obviously.

Figure 14 shows the crush deformation of regular pentagon paper corrugation tube along Y direction with different tube lengths. It is obvious that the deformation of specimen of C5-70-12 is mainly steady state progressive buckling, and there are a slight Euler buckling near the bottom of the

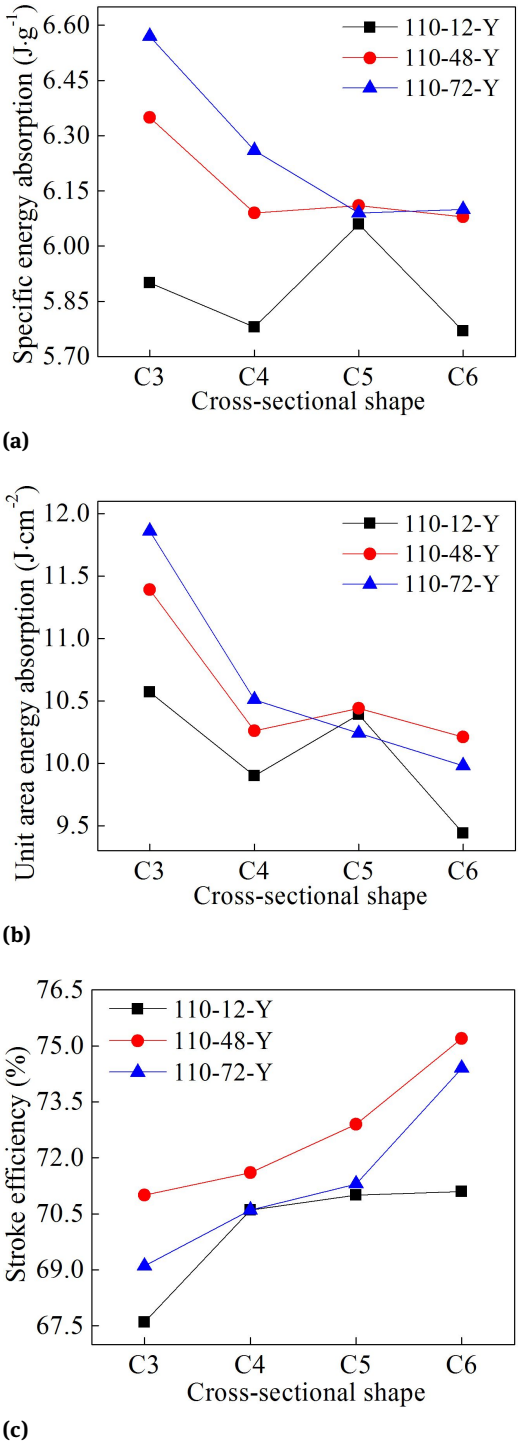

Figure 12: Effects of different cross-sectional shapes of paper corrugation tube along Y direction on cushioning energy absorption parameters: (a) specific energy absorption; (b) unit area energy absorption; (c) stroke efficiency

tube and a slight transverse shear phenomenon. For the specimen of C5-110-12, the steady state progressive buckling occurs firstly, and then the Euler buckling and transverse

Table 4: Cushioning energy absorption of regular pentagon paper corrugation tubes

Specimens	P_{max} (N)	P_m (N)	*SE* (%)	*E* (J)	*SEA* (J/g)	*S* (J/cm^2)	*CFE* (%)
C5-70-12-X	1135	865	61.8	37.0	1.66	1.76	76.2
C5-110-12-X	1300	880	64.4	62.1	1.76	2.96	67.7
C5-150-12-X	1130	876	64.5	83.9	1.74	4.00	77.5
C5-70-12-Y	2885	2559	66.4	138.1	5.78	6.58	88.7
C5-110-12-Y	3175	2841	71.0	218.2	6.04	10.39	89.5
C5-150-12-Y	3090	2664	73.1	288.3	5.92	13.73	86.2

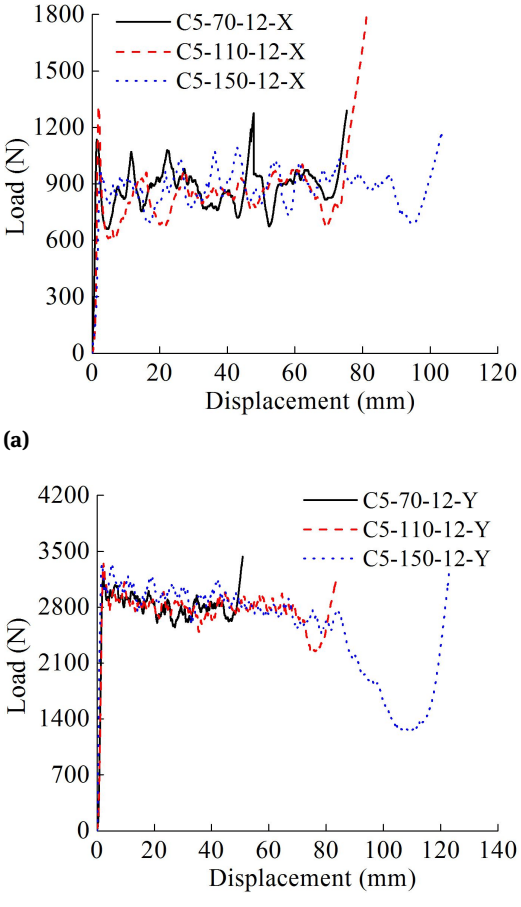

Figure 13: Load and displacement curves of regular pentagon paper corrugation tubes with different tube lengths: (a) tubes along X direction; (b) tubes along Y direction

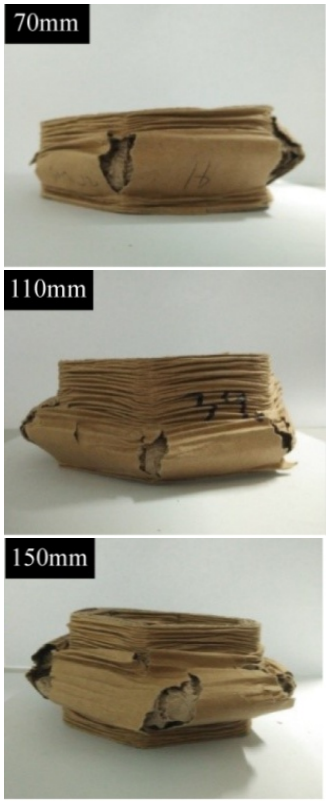

Figure 14: Crush deformation of regular pentagon paper corrugation tubes along Y direction with different tube lengths

shear occur. Meanwhile, its Euler buckling is more serious than that of the tube length with 70mm. Compared with specimens of C5-70-12 and C5-110-12, the Euler buckling of specimen of C5-150-12 is the most serious and the angular tear phenomenon occurs. For the tubes along Y direction, the increase of tube length causes the combined deformation modes more complex and reduces the bearing capacity of the structure.

The initial peak force and the mean crush force of regular pentagon paper corrugation tubes along X and Y direction with three kinds of length are illustrated in Figure 15. For the tube length of 110mm, both the initial peak force and the mean crush force are the largest. The results of energy absorbing characteristics with different tube lengths are shown in Figure 16. The total energy absorption, unit area energy absorption and stroke efficiency of tubes along X and Y direction all gradually improve, the reason are no change of bearing area and the increase of compressible distance. However, the change of the specific energy absorption is not obvious because the gross mass of the structure increase at the same time.

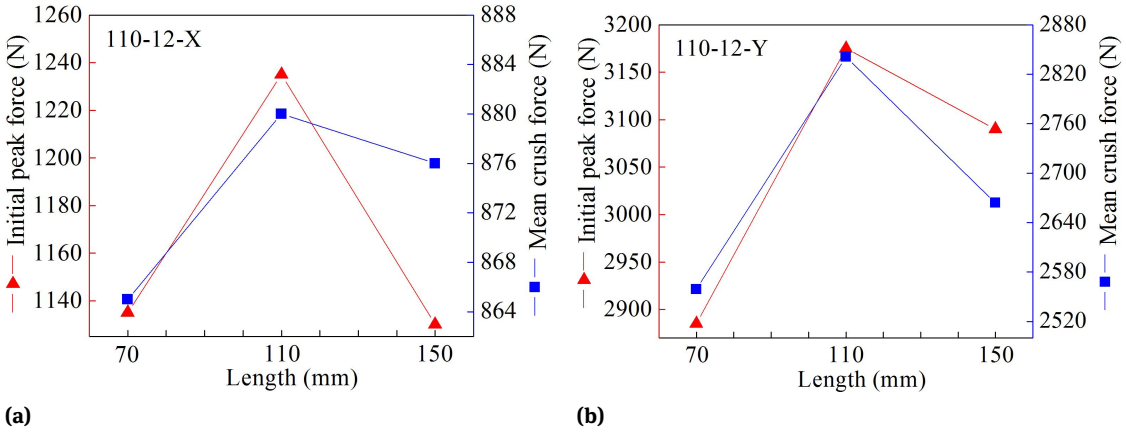

Figure 15: Initial peak force and mean crush force of regular pentagon paper corrugation tubes with different tube lengths: (a) tubes along X direction; (b) tubes along Y direction

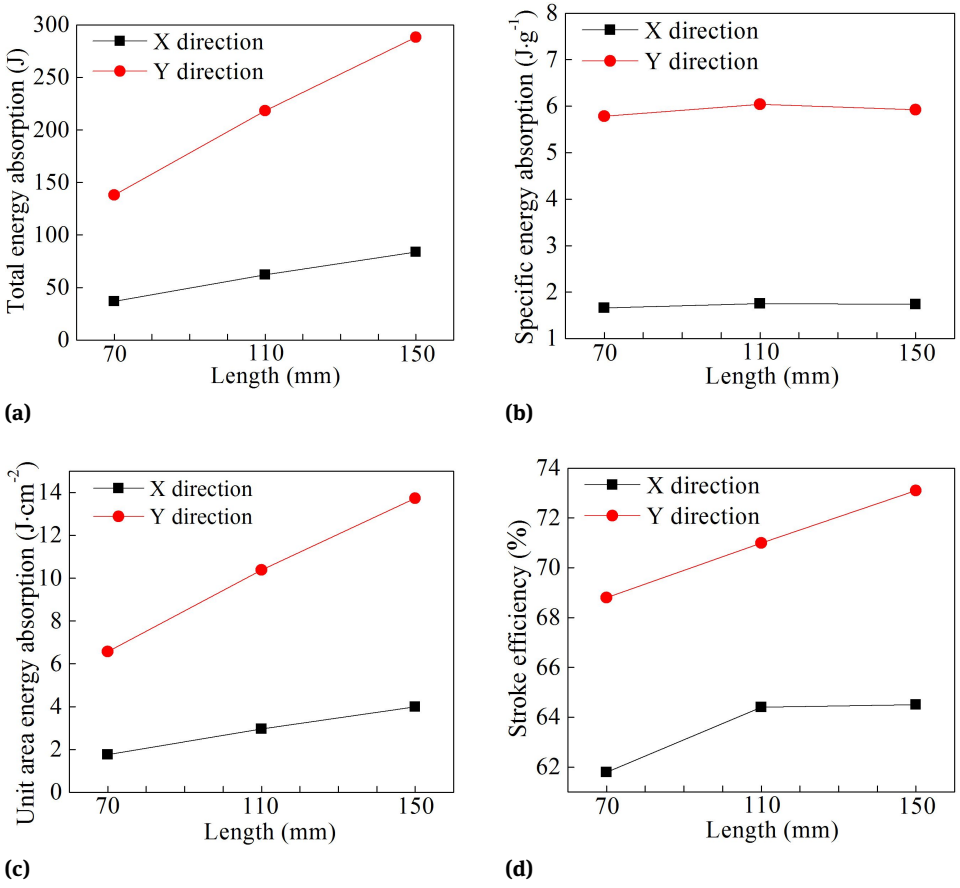

Figure 16: Effects of tube lengths of regular pentagon paper corrugation tube on cushioning energy absorption parameters: (a) total energy absorption; (b) specific energy absorption; (c) unit area energy absorption; (d) stroke efficiency

4.5 Effect analysis of compression rate

Figure 17 shows that the comparison of axial static compression load and displacement curves of regular pentagon paper corrugation tubes along X and Y direction with three kinds of compression rates. Combined with the results of cushioning energy absorbing parameters of tubes along X direction in Table 2, we can find that the total energy ab-

sorption, specific energy absorption and unit area energy absorption of tube along X direction gradually improve as the axial compression rates increasing. For the deformation modes of tube along Y direction, the cushioning energy absorption of steady state progressive buckling is more stable and more efficient than Euler buckling, angular tear and transverse shear. The steady state progressive buckling is an ideal energy absorbing mode, yet for the increase of compression rate, the non-ideal deformation modes of Euler buckling, angular tear and transverse shear are more likely to occur.

The four kinds of cushioning energy absorption parameters of paper corrugation tube along Y direction at different compression rates are displayed in Figure 18. The total energy absorption, specific energy absorption and unit area energy absorption of the regular triangle and quadrangle tubes along Y direction gradually increase with the rise of compression rates. However, those of the regular pentagon and hexagon tube along Y direction decrease when the compression rate is 72 mm/min. For the regular pentagon and hexagon paper corrugation tubes, the large

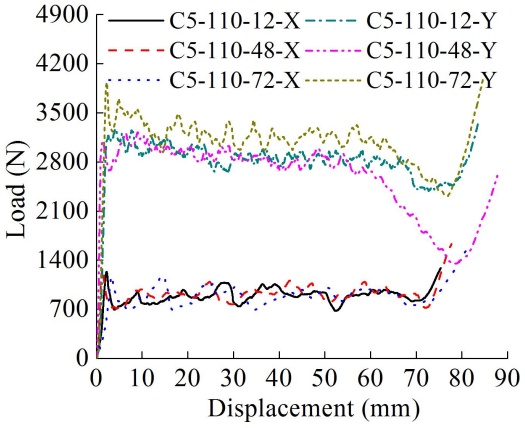

Figure 17: Load and displacement curves of paper corrugation tubes with different compression rates

compression rate results in the increase of contribution proportion of non-ideal deformation modes and decrease of the cushioning properties. Figure 18(d) shows that the stroke efficiency of tube along Y direction at compression rate of 48 mm/min is the largest. For the compression rate

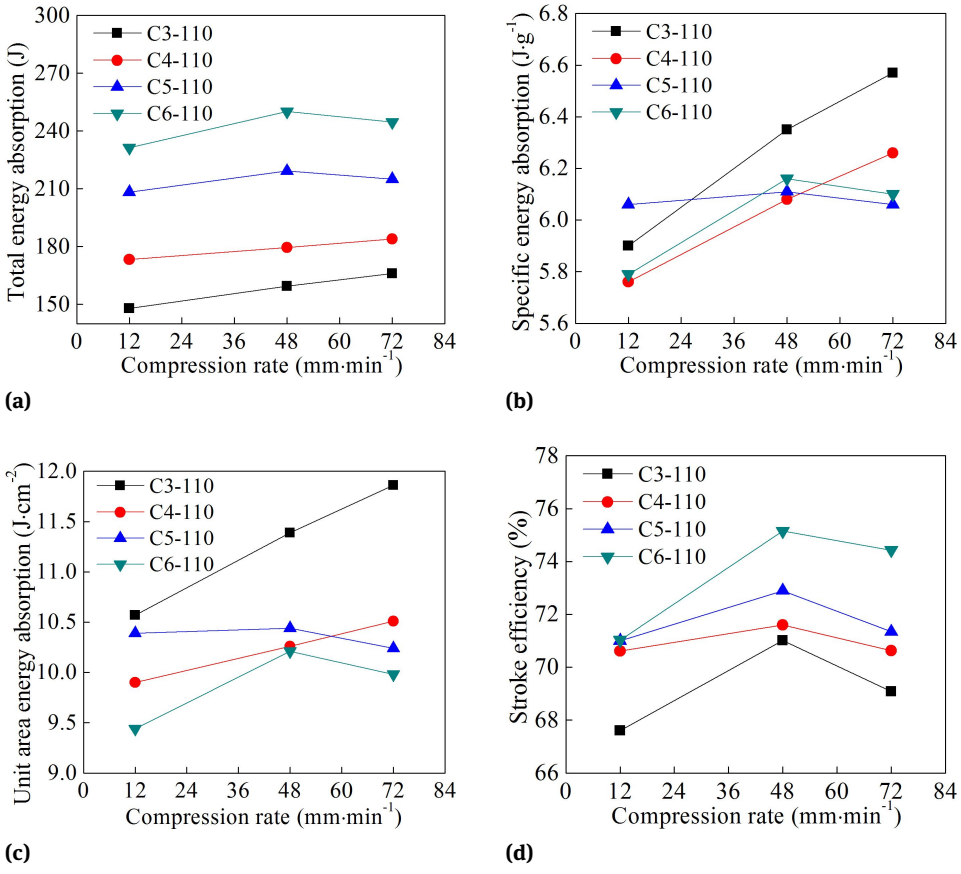

Figure 18: Effects of different compression rates on cushioning energy absorption parameters of paper corrugation tube along Y direction: (a) total energy absorption; (b) specific energy absorption; (c) unit area energy absorption; (d) stroke efficiency

increases to 72 mm/min, the stroke efficiency decreases as the change of the combination deformation modes.

5 Conclusions

The paper corrugation tube is an innovative kind of non-metallic tubular structure, and has an attractive engineering application for military and civilian product protection and packaging. In this paper, an improved folding element method is proposed to predict the mean crush force and the mechanical properties of regular polygon paper corrugation tubes under axial static compression were investigated. The total energy absorption, specific energy absorption, unit area energy absorption, crushing force efficiency and stroke efficiency were calculated, and the effects of different tube direction, cross-sectional shape, tube length and compression rate on failure modes and cushioning energy absorbing properties of regular polygon paper corrugation tubes were determined. The following conclusions are drawn:

(1) The paper corrugation tubes along X direction only occur stable and controllable accordion deformation mode, yet the paper corrugation tube along Y direction has four deformation modes including steady state progressive buckling, Euler buckling, angular tear and transverse shear. The effects of geometric parameters and compression rate on the accordion deformation mode of tubes along X direction are generally not significant, but it can affect the deformation proportion of tubes along Y direction between steady state progressive buckling and three kinds of non-ideal deformation modes.

(2) At the compression rates of 12 and 48 mm/min, the cushioning properties of the regular triangle and pentagon paper corrugation tubes along Y direction are better than that of the tubes with regular quadrangle and hexagon cross-sections. The stroke efficiency of paper corrugation tubes with two directions gradually rises with the increase of the side number of regular polygon. For the paper corrugation tubes along Y direction, when the tube length is 150 mm or compression rate is 72 mm/min, the bearing capacity and the cushioning energy absorbing properties of the structure are declined due to the increase of the contribution proportion of non-ideal deformation modes.

(3) The bearing capacity of paper corrugation tubes along Y direction is much higher than the tubes along X direction, because the axial compression load is applied along the direction of corrugation pillar of corrugated paperboard for tubes along Y direction but along corrugation wave of corrugated paperboard for tubes along X direction. Meanwhile, the total energy absorption, specific energy absorption, the crush force efficiency, unit area energy absorption and stroke efficiency of tubes along Y direction are all higher than those of the tubes along X direction. Thus the paper corrugation tube along Y direction has better cushioning energy absorbing properties.

Acknowledgement: The work was supported by the National Natural Science Foundation of China (grant number 51345008), the Foundation of Xi'an Science and Technology Bureau (grant number 2017080CG/RC043), the Foundations of Shaanxi Province Science and Technology Department (grant numbers 2017ZDCXL-GY-02-01 and 2018GY-191).

References

[1] Lakes R. Materials with structural hierarchy. Nature 1993;361(11):511-515.

[2] Kooistra GW, Deshpande V, Wadley HNG. Hierarchical corrugated core sandwich panel concepts. Journal of Applied Mechanics 2007;74(1):259-268.

[3] Hohe J, Becker W. Effective stress-strain relations for two-dimensional cellular sandwich cores: Homogenization, material models, and properties. Applied Mechanics Review 2002;55(1):61-87.

[4] Kazemahvazi S, Tanner D, Zenkert D. Corrugated all-composite sandwich structures. Part 2: Failure mechanisms and experimental programme. Composites Science and Technology 2009;69:920-925.

[5] Lu TJ, Chen C, Zhu G. Compressive behavior of corrugated board panels. Journal of Composite Materials 2001;35(23):2098-2126.

[6] Krusper A, Isaksson P, Gradin P. Modeling of out-of-plane compression loading of corrugated paper board structures. Engineering Mechanics 2007;133(11):1171-1177.

[7] Rami HA, Choi J, Wei BS, et al. Refined nonlinear finite element models for corrugated fiberboards. Composite Structures 2009;87(4):321-333.

[8] Talbi N, Batti A, Ayad R, *et al.* An analytical homogenization model for finite element modeling of corrugated cardboard. Composite Structures 2009;88 (2):280-289.

[9] Sek MA, Kirkpatrick J. Prediction of the cushioning properties of corrugated fiberboard from static and quasi-dynamic compression data. Packaging Technology and Science 1997;10(2):87-94.

[10] Sek M, Rouillard V, Tarash H, *et al.* Enhancement of cushioning performance with paperboard crumple inserts. Packaging Technology and Science 2005;18(5):273-278.

[11] Gao D, Wang ZL, Chen NL, *et al.* The dynamic modeling of flat compression cushioning made up of B-flute double-wall corrugated fiberboard. Journal of Vibration Engineering 2001;14(2):172-178. (In Chinese)

[12] Zhu DP, Zhou SS. Dynamic modeling and response analysis of corrugated paperboard to shock excitation. Mechanical Science and Technology for Aerospace Engineering 2013;32(2):257-262.

(In Chinese)
[13] Wang DM. Cushioning properties of multi-layer corrugated sandwich structures. Sandwich Structures and Materials 2009;11(1):57-66.
[14] Guo YF, Xu WC, Fu YG, *et al.* Dynamic shock cushioning characteristics and vibration transmissibility of X-PLY corrugated paperboard. Shock and Vibration 2011;18(4):525-535.
[15] Guo YF, Xu WC, Fu YG, et al. Comparison studies on dynamic packaging properties of corrugated paperboard pads. Journal of Engineering 2010;2(5):378-386.
[16] Guo YF, Becker W, Fu YG, *et al.* Package cushioning properties of corrugated paperboard pads with hollow pillars. In: Proceedings of 2^{nd} International Conference on Packaging Technology and Science. Wuxi, China; 2014.
[17] Kılıçaslan C, Güden M, Odacı İK, *et al.* The impact responses and the finite element modeling of layered trapezoidal corrugated aluminum core and aluminum sheet interlayer sandwich structures. Materials and Design 2013;46:121-133.
[18] Qiu XM, Pan ML, Yu XH, *et al.* Analysis of the energy absorption properties for tubular structure under axial compression of different failure models. Mechanics in Engineering 2016;38(5):477-492. (In Chinese)
[19] Eyvazian A, Habibi MK, Hamouda AM, *et al.* Axial crushing behavior and energy absorption efficiency of corrugated tubes. Materials and Design 2014;54:1028-1038.
[20] Liu ZF, Hao WQ, Xie JM, *et al.* Axial-impact buckling modes and energy absorption properties of thin-walled corrugated tubes with sinusoidal patterns. Thin-Walled Structures 2015;94:410-423.
[21] Xiong J, Feng LN, Ghosh R, *et al.* Fabrication and mechanical behavior of carbon fiber composite sandwich cylindrical shells with corrugated cores. Composite Structures 2015;156:307-319.
[22] Kılıçaslan C. Numerical crushing analysis of aluminum foam-filled corrugated single-and double-circular tubes subjected to axial impact loading. Thin-Walled Structures 2015;96:82-94.
[23] Wierzbicki T, Abramowicz W. On the Crushing Mechanics of Thin-Walled Structures[J]. Journal of Applied Mechanics, 1983;50(4):727-734.